Using Redox Switchable Polymerization Catalysis to Synthesize a Chemically Recyclable Thermoplastic Elastomer

Jiangwei Liu,[a] Sarah E. Blosch,[b] Anastasia S. Volokhova,[b] Erin R. Crater,[b] Connor F. Gallin,[a] Robert B. Moore,[b] John B. Matson*,[b] Jeffery A. Byers*[a]

Dedicated to the late Professor Jeffery A. Byers for his outstanding contributions to the fields of catalysis and polymer synthesis.

[a] J. Liu, C. F. Gallin, Prof. J. A. Byers
Department of Chemistry, Boston College,
Eugene F. Merkert Chemistry Center
2609 Beacon Street, Chestnut Hill, MA 02467 (USA)

[b] S. E. Blosch, A. S. Volokhova, E. R. Crater, Prof. R. B. Moore, Prof. J. B. Matson
Department of Chemistry,
Virginia Tech Center for Drug Discovery, and Macromolecules Innovation Institute, Virginia Tech
Blacksburg, VA 24061 (USA)
E-mail: jbmatson@vt.edu

Supporting information for this article is given via a link at the end of the document.

Abstract: In an effort to synthesize chemically recyclable thermoplastic elastomers, a redox-switchable catalytic system was developed to synthesize triblock copolymers containing stiff poly(lactic acid) (PLA) end-blocks and a flexible poly(tetrahydrofuran-*co*-cyclohexene oxide) (poly(THF-*co*-CHO) copolymer as the mid-block. The orthogonal reactivity induced by changing the oxidation state of the iron-based catalyst enabled the synthesis of the triblock copolymers in a single reaction flask from a mixture of monomers. The triblock copolymers demonstrated improved flexibility compared to poly(L-lactic acid) (PLLA) and thermomechanical properties that resemble thermoplastic elastomers, including a rubbery plateau in the range of -60 to 40 °C. The triblock copolymers containing a higher percentage of THF versus CHO were more flexible, and a blend of triblock copolymers containing PLLA and poly(D-lactic acid) (PDLA) end-blocks resulted in a stereocomplex that further increased polymer flexibility. Besides the low cost of lactide and THF, the sustainability of this new class of triblock copolymers was also supported by their depolymerization, which was achieved by exposing the copolymers sequentially to $FeCl_3$ and $ZnCl_2$/PEG under reactive distillation conditions.

Introduction

Over the past decade, switchable catalysis,[1,2] where a single catalyst can toggle between two or more catalytic cycles through application of an external stimulus,[3–20] has emerged as a novel strategy to synthesize block copolymers. The temporal control inherent to these reactions enables one-pot syntheses of complicated multiblock copolymer structures from a mixture of monomers with sequence that is defined by the time when the external stimulus is applied.[20–26] This aspect overcomes the limitation of copolymerization reactions that are dictated by reactivity ratios innate to monomers,[27–34] and circumvents the tedious post-polymerization chain-end modifications often required to obtain block copolymers.[24,31] Despite the complexity and tunability that can be added to polymer structures, the use of switchable polymerization for synthesizing engineering polymers has remained underexplored.[2] Limited examples use switchable catalysis to obtain thermoplastic elastomers (TPEs),[4,21,35] pressure-sensitive adhesives,[35,36] or toughened plastics.[35]

Previously, our group reported a redox switchable polymerization system facilitated by a set of bis(imino)pyridine iron alkoxide complexes (Scheme 1).[9,10] When this complex is in the iron(II) oxidation state (i.e., complex **1**), L-lactide (*L*-LA) can be polymerized with living characteristics into poly(*L*-lactic acid) (PLLA). Upon oxidation, the cationic iron(III) complex **2** is generated, which arrests the conversion of *L*-LA and is activated for epoxide polymerization. The orthogonal reactivity of **1** and **2** toward lactide and epoxide, respectively, enabled the synthesis of poly(ester-*b*-ether) block copolymers.[9] While this example of switchable catalysis demonstrated how redox-switchable polymerization could be used to synthesize block copolymers, the resulting copolymers did not have useful mechanical properties.

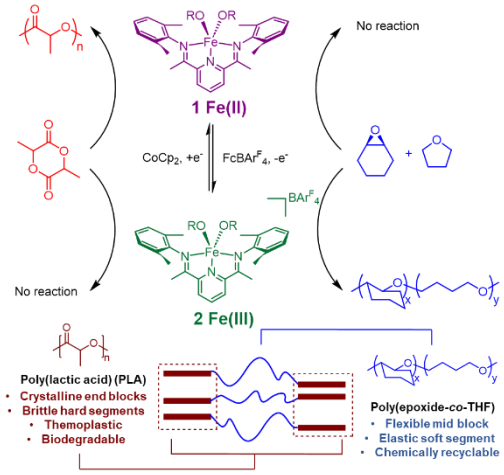

Scheme 1. Redox switchable copolymerization catalyzed by bis(imino)pyridine iron alkoxide complexes.

Inspired by research from Hillmyer and coworkers, who synthesized triblock copolymers that were useful TPEs[37–41] featuring semicrystalline PLLA end-blocks and flexible biobased polyester mid-blocks, we targeted the synthesis of TPEs that contained PLLA end-blocks using our redox-switchable polymerization strategy. We identified poly(tetrahydrofuran) (poly(THF)) as a potentially useful mid-block for a TPE because it is a flexible polyether with high abrasion resistance.[42–46] It has a glass-transition temperature (T_g) of -83 °C[47], making it a useful soft block in segmented polyurethane TPEs like Spandex.[48] While it has a T_m of 41 °C, not ideal for a TPE soft block, we envisioned that the crystallinity could be largely disrupted by incorporating a small amount of a comonomer.[42] Moreover, poly(THF) has a low ceiling temperature, and can be readily depolymerized to THF using $FeCl_3$ as a catalyst.[49] Given the propensity for PLLA to undergo depolymerization under reactive distillation conditions,[50–55] we envisioned that chemical recycling of both components of the TPE could be achieved under similar conditions. Although polymers with low ceiling temperature have been used as hard or soft segments in TPEs,[56–58] full depolymerization of a triblock copolymer back to its constituent monomers has never been reported. Considering that TPEs are used for many single-use applications, developing a chemically recyclable TPE derived from commodity monomers would be a valuable step forward for a circular plastic economy.

Results and Discussion

Table 1. Molecular weight and composition of THF/CHO copolymer synthesized at various feed ratios, solvents, and concentrations.[a]

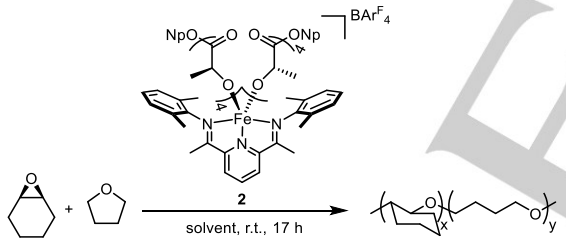

Entry	$[CHO]_0$: $[THF]_0$[b]	Solvent	[THF] (M)	M_n (kg/mol)[c]	$Đ$[c]	F_{THF}[d]	Yield (%)[f]
1	2500:500	CH_2Cl_2	0.25	21.6	2.46	0.12	76 (84)
2	500:500	CH_2Cl_2	0.25	14.8	2.14	0.30	53 (75)
3[e]	500:2500	CH_2Cl_2	0.50	11.7	2.18	0.41	12 (60)
4	5:25000	THF	12.3	83.8	2.60	0.78	20 (72)
5	500:25000	CH_2Cl_2	6.16	19.6	1.92	0.79	22 (77)
6	50:10000	CH_2Cl_2	6.16	8.50	1.73	0.92	18 (71)
7	50:10000	PhMe	6.16	20.9	1.94	0.97	22 (79)
8	50:10000	PhCl	6.16	25.8	1.72	0.94	24 (76)
9	250:2500	PhCl	3.08	30.9	1.49	0.62	38 (80)

[a] NpO = neopentoxy group, BAr$^F_4$ = tetrakis(3,5-bis(trifluoromethyl)phenyl) borate. [b] Equiv relative to Fe complex (**2**). [c] Molecular weights and $Đ$ values were determined from the signal response of the refractive index (RI) detector on a size exclusion chromatography (SEC) system relative to polystyrene standards. [d] Mol fraction of polyTHF in the copolymer. [e] Reaction ran for 48 h. [f] Isolated yield (yield based on recovered starting material).

Considering that the iron(III) complex **2** was active for epoxide ring-opening polymerization in our original redox-switchable polymerization system,[9] we thought it might be active for THF ring-opening polymerization. However, initial attempts to polymerize THF without comonomer catalyzed by **2** failed. Nevertheless, when cyclohexene oxide (CHO) polymerization was carried out in THF as the solvent, the reaction mixture formed a gel within an hour. Proton nuclear magnetic resonance spectroscopy (^{1}H NMR) revealed that the polymer was a copolymer containing poly(CHO) and poly(THF). These results indicated that poly(THF) formation required an epoxide as a comonomer, a relatively common occurrence for THF polymerization.[42,43,59,60] To avoid gelation, we next explored CHO/THF copolymerization reactions in CH_2Cl_2 (Table 1, Table S1). A reaction run with an excess of CHO consumed both monomers efficiently (solid lines, Figure 1), and resulted in a moderate molecular weight polyether (M_n = 21.6 kg/mol) containing 12 mol% THF (Table 1, entry 1, Figures S1–2). Increasing THF in the feed led to slower reaction rates (dotted lines, Figure 1) and lower molecular weights but with substantially more THF incorporation (Table 1, entries 2-3, Figures S3-7). All the copolymers obtained had molecular weights that were not linearly correlated with conversion and had broad molecular weight distributions, suggesting uncontrolled chain polymerization, similar to CHO homopolymerization catalyzed by **2**.[9]

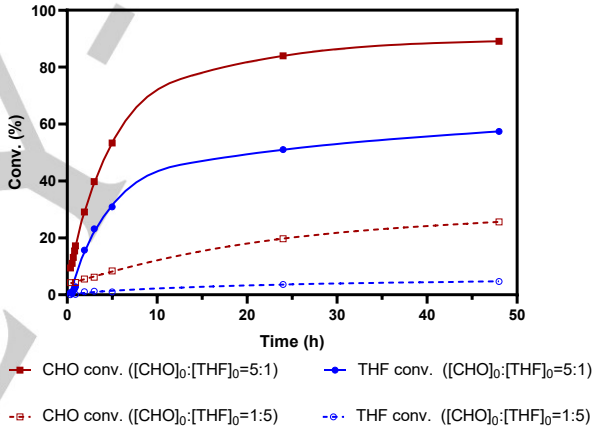

Figure 1. Time course Studies of THF/CHO copolymerization were performed in CD_2Cl_2 as solvent in J. Young tubes at rt. THF (blue circles) and CHO (red squares) conversion over time at [CHO]: [THF] = 5:1 (solid symbols/solid line) and 1:5 (open symbols/dotted line).

Attempting to synthesize THF-enriched copolymers, we next performed the reaction in neat THF (Table 1, entry 4, Figures S8-9). As expected, a gel formed 17 h after adding 5 equiv. CHO into a THF solution containing **2**. Although high conversion was inhibited by the high viscosity of the reaction mixture, ^{1}H NMR analysis of the copolymer revealed 78% THF incorporation. The low isolated yield was due to a large excess of unreacted THF, which can be easily recycled by distillation. To lower reaction viscosity, CH_2Cl_2 was added to the reaction mixture while maintaining relatively high THF concentrations ($[THF]_0$ = 6.16 M) and a large excess of THF in the feed ($[CHO]_0$: $[THF]_0$ = 1:50). Satisfyingly, these conditions led to polymerization without gelation, and the obtained copolymer incorporated nearly the same amount of THF (79%) as the reaction carried out in neat THF (Table 1, entry 5, Figure S10–11). Compared to the reaction in neat THF, the molecular weight of this copolymer was smaller with a narrower dispersity. Maintaining the THF concentration while increasing the feed ratio of $[CHO]_0$: $[THF]_0$ to 1:200 led to even higher THF incorporation in the copolymer (Table 1, entry 6,

Figures S12–13). Finally, altering the solvent revealed that toluene (PhMe) was the best solvent for high THF incorporation (Table 1, entry 7, Figures S14–15), while chlorobenzene (PhCl) led to the highest molecular weight copolymer compared with other solvents (Table 1, entry 8, Figure S16-17). As was the case in CH_2Cl_2, the amount of THF incorporated in the copolymer produced in PhCl could be modified by altering the THF concentration and $[CHO]_0$: $[THF]_0$ ratio (Table 1, entry 9, Figures S18–19). Considering these findings, we reasoned that tuning the molecular weight of the copolymer was best achieved by altering the identity of the solvent, and controlling the composition in the copolymer was best achieved by altering the feed ratio.

Having established a useful method to polymerize THF with catalyst **2**, we next set out to synthesize A-B-A' triblock copolymers containing PLLA end-blocks and a polyether mid-block using redox-switchable polymerization. To do so, we explored reactions containing a mixture of *L*-LA, THF, and CHO (Figure 2, S20). Starting with iron(II) complex **1**, *L*-LA was polymerized for 10 min to give a narrowly distributed PLLA block without any evidence for THF or CHO conversion (M_n = 7.9 kg/mol; $Đ$ = 1.17). The oxidant ferrocenium tetrakis(3,5-bis(trifluoromethyl) phenyl) borate ($FcBAr^F_4$) was then added to the reaction mixture, which converted the catalyst into an iron(III) complex, halting *L*-LA polymerization and initiating CHO/THF copolymerization. After 3 h, a polyether block derived from CHO and THF was installed as the second block with an increase in molecular weight and dispersity (M_n = 14.1 kg/mol; $Đ$ = 1.78). Finally, the last block of the triblock copolymer was installed by adding the reductant decamethyl cobaltocene ($CoCp^*_2$) to the reaction mixture, which resulted in polymerizing the remaining *L*-LA to produce the A-B-A' triblock copolymer (M_n = 18.5 kg/mol; $Đ$ = 1.68). Notably, isolation of the triblock copolymer and analysis by diffusion-ordered spectroscopy (DOSY) showed a single diffusing species consistent with the ABA triblock copolymer product (Figure S21).

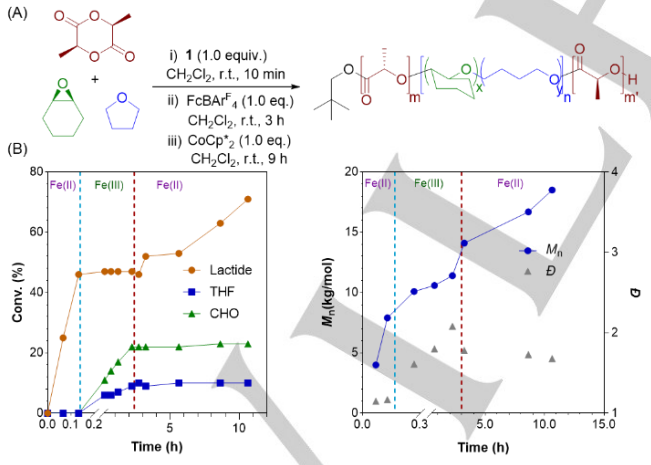

Figure 2. (A) Scheme of redox-switchable copolymerization of THF, CHO and *L*-LA. (B) Monomer conversion vs. time (top), and M_n, and $Đ$ vs. time (bottom). The oxidation state of the catalyst in each step is represented at the top of each plot with vertical lines indicating the addition of redox reagents in steps ii) and iii). The neopentoxy group (NpO) in the polymer structure was from the iron catalyst and the initiator.

Next, we targeted the synthesis of various A-B-A' triblock copolymers. Because the effect of the end-block to mid-block ratio on the properties of triblock copolymers used as TPEs has been well studied,[37] we focused on synthesizing triblock copolymers with various THF incorporation in the polyether segment while keeping the relative length of each end-block to mid-block roughly constant at ~1:2. Adapting the optimal conditions developed for THF/CHO copolymerization from Table 1, we were able to synthesize a small library of PLLA-*b*-poly(THF-*co*-CHO)-*b*-PLLA (L-THF-L) triblock copolymers containing similar end-block: mid-block ratios and polymer segment molecular weights but significantly different THF incorporation in the mid-block (Table 2). Polymerizations conducted in CH_2Cl_2 allowed for the synthesis of a triblock copolymer containing 30% THF repeating units in the mid-block (Table 2, entry 1, Figures S22–27), but the synthesis of a triblock copolymer with a THF-enriched mid-block of the desired length was not possible in this solvent. We then moved to PhCl for preparing triblock copolymers with high THF incorporation. Notably, the necessity of high THF concentrations for high THF incorporations in the mid-block led to complications due to the low solubility of *L*-LA in THF/PhCl mixtures. To overcome this obstacle, the *L*-LA required for the first block was reacted to full conversion, and then a second portion of *L*-LA was added during the third step of the reaction (Table 2, entries 2-3, Figures S28–40). As expected, D-lactide (*D*-LA) could be included in the triblock copolymer instead of *L*-LA without significant difference to give PDLA-*b*-poly(THF-*co*-CHO)-*b*-PDLA (D-THF-D, Table 2, entry 4, Figures S41–46).

Table 2. (A) Scheme of redox-switchable polymerization between THF, CHO and *L*-LA. (B) M_n, and $Đ$ after each step and F_{THF} in the second step[a]

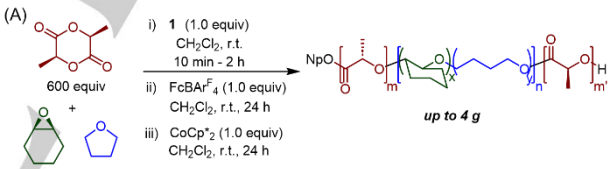

(B)

		After step i)			After step ii)				After step iii)			
	$[CHO]_0$: $[THF]_0$	$M_{n,SEC}$[a] (kg/mol)	$M_{n,NMR}$[a] (kg/mol)	$Đ$	$M_{n,SEC}$[a] (kg/mol)	$M_{n,NMR}$[a] (kg/mol)	$Đ$	F_{THF}[b]	$M_{n,SEC}$[a] (kg/mol)	$M_{n,NMR}$[a] (kg/mol)	$Đ$	Yield (%)[h]
1	500:500[c]	32.3	35.0	1.08	59.3	69.8	1.69	0.30	87.1	99.2	1.19	40 (78)
2	250:2500[d,e]	28.9	24.3	1.08	70.2	51.7	1.83	0.68	99.3	76.3	1.49	28 (64)
3	50:10000[d,e]	28.5	28.5	1.14	74.1	70.3	1.65	0.95	107.7	94.7	1.52	10 (72)
4	50:10000[d,f]	31.0	30.5	1.10	77.1	65.1	1.60	0.96	111.1	89.8	1.35	10 (70)
5	50:10000[d,g]	28.9	31.4	1.06	77.1	80.6	1.68	0.96	107.1	99.8	1.39	11 (76)

[a] $M_{n,SEC}$ values were determined by SEC equipped with a light scattering detector; $M_{n,NMR}$ values were determined based on end-group analysis using the neopentyl end group signal. [b] THF mole fraction in mid-block copolymer, determined by ^{1}H NMR. [c] The conversion of *L*-LA was controlled at ~50% in the 1st step by letting it react for 10 min. The total equiv of LA added is shown in the reaction scheme; cobaltocene ($CoCp_2$) used as reductant. [d] *L*-LA was added twice in the 1st and 3rd step. [e] Reaction performed in PhCl. CH_2Cl_2 was added in the 3rd step to reduce viscosity. [f] *D*-LA was added instead in the 1st and 3rd step. [g] *D*-LA was added instead in the 3rd step. [h] Isolated yield (yield based on recovered starting material).

Coupling the sequential addition of lactide with the ability to incorporate *L*-LA and *D*-LA, we synthesized an A-B-C triblock copolymer PLLA-*b*-poly(THF-*co*-CHO)-*b*-PDLA (L-THF-D) containing PLLA and PDLA end-blocks (Table 2, entry 5, Figures S47–50). This polymer was interesting because it features end-blocks that are expected to form stereocomplexes, a well-known property displayed by mixtures of PLLA and PDLA.[61] Notably, the accessibility of the L-THF-D is enabled using the unidirectional, redox-switchable polymerization method employed as opposed to

conventional bidirectional, telechelic techniques used to synthesize triblock copolymers containing PLLA end-blocks.[37–41,62–66] All copolymers were isolated on a multi-gram scale and were confirmed to be triblock copolymers as determined by ^{1}H NMR, SEC, and DOSY spectroscopy (See Figure S22-50).

We next evaluated the thermal properties of the blend between L-THF-L (Table 2, entry 3) and D-THF-D (Table 2, entry 4) along with L-THF-D (Table 2, entry 5) to see if they could form stereocomplexes. Samples were prepared using similar methods to those previously reported for PLLA/PDLA stereocomplexes.[67] Thermal analysis revealed a higher melting temperature (T_m) in the differential scanning calorimetry (DSC) thermograph (Figure 3) for the blend of L-THF-L and D-THF-D (T_m = 224 °C) compared to L-THF-L (T_m = 178 °C). The 46 ºC increase in T_m for the triblock copolymer blend was similar to what has been observed in blends of PLLA/PDLA.[67] In comparison, L-THF-D displayed a lower melting point (T_m = 213 °C) than the triblock copolymer blends, but a higher melting point than pure L-THF-L. This outcome indicated that the A-B-C triblock copolymer also formed a stereocomplex, yet different than what was observed from A-B-A' triblock copolymer blends. This may result from varying amounts of D- and L-lactide repeat units in the A-B-C triblock copolymer, where SEC results show a small excess of D-lactide units. The T_m value for the poly(THF-*co*-CHO) mid-block in the A-B-A' triblock copolymer blend (43 °C) and the A-B-C triblock copolymer (32 °C) were slightly higher than pure L-THF-L or D-THF-D (26–27 °C). This suggests that while the primary intermolecular interactions in the triblock copolymer blends and A-B-C triblock copolymer are between the PLA end-blocks, the mid-blocks were also affected.

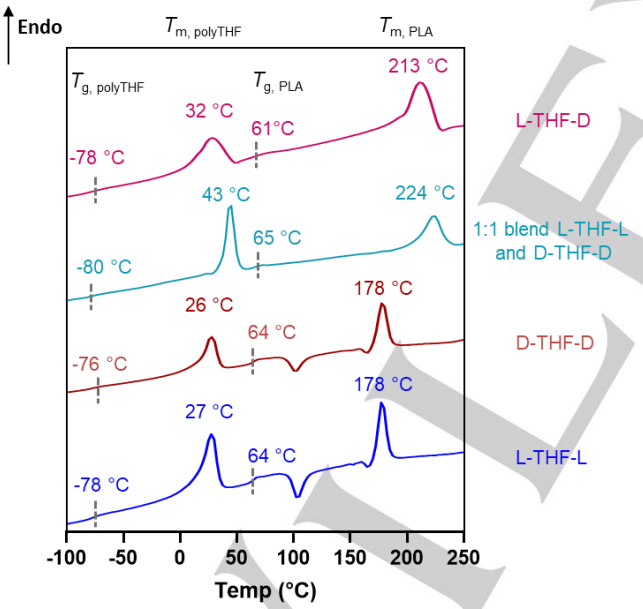

Figure 3. DSC thermographs of triblock copolymers and the stereocomplex blend: L-THF-L is PLLA-*b*-poly(THF-*co*-CHO)-*b*-PLLA (Table 2, entry 3); D-THF-D is PDLA-*b*-poly(THF-*co*-CHO)-*b*-PDLA (Table 2, entry 4), and L-THF-D is PLLA-*b*-poly(THF-*co*-CHO)-*b*-PDLA (Table 2, entry 5). All polymers have a ≥95% enrichment of THF in the mid-block. DSC thermographs of L-THF-D and the blend were from the 1st heating cycle at a heating rate of 20 K/min; others were from the 2nd heating cycle. Crystallization temperatures (T_c) were observed in DSC thermographs of L-THF-L (T_c = 103 ºC) and D-THF-D (T_c = 101 ºC) but absent in the blend and L-THF-D.

With a library of triblock copolymers in hand, we assessed the mechanical properties of these materials by uniaxial tensile testing and dynamic mechanical analysis (DMA) (Table 3, Figure 4). Compared with pristine PLLA,[68,69] the triblock copolymers had a greater strain at break. This fact was true regardless of THF content in the mid-block (*c.f.*, entry 1 to entries 2–6). In contrast to the polymer flexibility, Young's moduli for the triblock copolymers were consistently much lower than pristine PLLA, a common observation when amorphous mid-blocks are inserted in crystalline end-blocks in triblock copolymers.[40] When the THF fraction in the mid-block increased from 30% to 68%, the ultimate tensile strain stayed around 30% elongation at break, while the modulus decreased more than 100 times (entries 2-3). A substantial change in material flexibility occurred when the THF fraction in the mid-block was 95% or greater, where the triblock copolymers showed more elastomeric behavior, reaching greater than 150% elongation at break in most samples (entries 4–5). The significant divergence in the mechanical behavior suggested that the ratio between THF and CHO in the copolymer can be used as a handle to tune the mechanical properties of the polymer.

Table 3. Comparison of mechanical properties between PLLA and triblock copolymers.[a]

Entry	Structure	M_n (kg/mol)[b]	F_{THF} [c]	σ_b (MPa)	ε_b (%)	E (MPa)	U_T (MPa)
1[d]	PLLA	100	N/A	50	3.3	2700	-
2	L-THF-L	32-27-32	0.30	12 ± 4	30 ± 20	1300 ± 80	570 ± 370
3	L-THF-L	29-41-29	0.68	12 ± 1	31 ± 10	6.8 ± 1.0	370 ± 120
4	L-THF-L	29-46-34	0.95	16 ± 3	277 ± 36	0.21 ± 0.01	2600 ± 670
5	D-THF-D	31-46-34	0.96	19 ± 2	154 ± 16	0.82 ± 0.10	2110 ± 380
6	Blend[e]	-	-	19 ± 3	324 ± 61	0.53 ± 0.10	3800 ± 930

[a] Entries 2-5 were the same polymer samples reported in Table 2, entries 1-4 in the same order. σ_b: tensile stress at break; ε_b: tensile strain at break; E: Young's modulus; U_T: toughness calculated by the area below curves. [b] Numbers represent M_n for each block of the copolymer in kg/mol as determined from SEC equipped with a light scattering detector. [c] THF mole fraction in copolymer, determined by ^{1}H NMR spectroscopy. [d] Data obtained from ref [69]. [e] blend of polymers from entries 4 and 5.

Of note, there was some batch-to-batch variability in the mechanical properties of the A-B-A' triblock copolymers synthesized (e.g., Table 3, entries 4-5), likely due to the T_m from mid-blocks that was close to room temperature, such that small changes in processing and measurement temperature affect the results. Despite some variability, the trend is clear that high THF content in these polymers affords flexible and tough TPEs, where toughness (U_T) is indicated by the area under the stress-strain curve. Moreover, the stereocomplex blend of copolymers (entry 6, Figures S51–53) showed higher flexibility (ε_b = 324 ± 61%) than either of the components in the blend, making it comparable to the properties of commercial melt processable rubbers.[70] While a PLA stereocomplex would increase the processing temperature required for these materials, studies on related PLA-based TPEs have shown some advantages in mechanical properties over TPEs with only PLLA hard blocks.[71] In contrast to the translucent and flexible films from the A-B-A' triblock copolymer films (L-THF-L or D-THF-D copolymers), the films of the A-B-C triblock copolymer L-THF-D sample were opaque and brittle. The films did not have suitable integrity to allow for mechanical properties testing. We speculate that intramolecular stereocomplexes possible with this A-B-C triblock copolymer prevented complete dissolution before the drop-casting process used to make the films, which resulted in opaque materials that

were too brittle to enable evaluation of their mechanical properties. This may also explain the lower melting point observed.

The DMA results for all the triblock copolymers synthesized had similar features to one another (Figures S27, 33, 40, 46, 53), but the ranges of the transitions changed with varying THF content in the mid-block. In samples with >95% THF content, two transitions were observed in all samples, near -60 and 40 °C, consistent with the T_g from the middle and end-blocks. The rubbery plateau, typically seen in TPEs,[72] was observed between -60 and 40 °C for these polymers. X-ray scattering studies of two selected films (L-THF-L and D-THF-D) revealed a morphology dominated by the phase separation of the semicrystalline PLLA or PDLA blocks. Intracrystalline reflections of the crystalline PLLA or PDLA segments were present in the wide-angle region, and the intercrystalline long periods of PLLA and PDLA, related to the averaged distance between PLLA or PDLA crystallites, were present in the SAXS region (Figure S54). This morphology is consistent with that of a similar triblock copolymer, PLLA-*b*-PEG-*b*-PLLA, reported in the literature.[73]

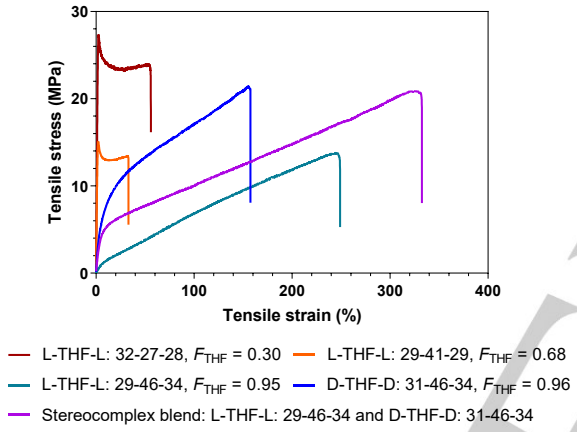

Figure 4. Stress-strain curves from uniaxial tensile testing of A-B-A' triblock copolymers L-THF-L with different THF incorporation in the mid-block and stereocomplexed A-B-A' triblock copolymer blend. Numbers represent the molecular weight of each block in kg/mol, as determined by SEC equipped with a light scattering detector.

Finally, in an effort to demonstrate that the new TPEs could be chemically recycled, we explored the depolymerization of L-THF-L. Enthaler and coworkers[49] reported poly(THF) with M_n up to 2.0 kg/mol can be depolymerized to THF at 160 °C with up to 90% yield using $FeCl_3$ as a Lewis acid catalyst.[49] Inspired by this work, we investigated whether the high molecular weight poly(THF-*co*-CHO) we synthesized could depolymerize in a similar fashion. Using a reactive distillation setup to recover THF from the depolymerization, initial attempts to depolymerize the poly(THF-*co*-CHO) copolymer (F_{THF} = 0.98, M_n = 108 kg/mol, $Đ$ = 1.52) were undertaken at 160 °C in the presence of 10 wt% $FeCl_3$ at 0.1 torr (Table S2, entry 1). Satisfyingly, this reaction resulted in 82% recovery of THF after 2 h and a near quantitative mass recovery (96%, including the 10 wt% $FeCl_3$ and small amounts of non-volatile oligomers). ^{1}H NMR analysis of the distilled product revealed <5% of an undetermined product, which we hypothesized came from CHO degradation. Lowering the reactive distillation temperature to 100 °C did not affect THF yield, but further decreasing the reactive distillation to 50 °C led to significantly diminished yields (Table S2, entries 2-3).

Encouraged by the success of mid-block depolymerization, we were interested in depolymerizing the triblock copolymer L-THF-L (Table S3, Figures S55–64). To begin with, we used $FeCl_3$ as the Lewis acid catalyst at 160 °C (Figure 5, column 1). THF yield was only slightly diminished compared to the polyether copolymer alone, but only 20% *L*-LA was recovered from the distillation. Recently, we discovered that the combination of $ZnCl_2$/PEG-600 (PEG = polyethylene glycol) can efficiently depolymerize many polyesters, including PLLA under similar reactive distillation conditions.[74] Therefore, we investigated the possibility of carrying out the depolymerization of the triblock copolymers in the presence of both catalysts (Figure 5, column 2). Improved yields were obtained for the recovery of *L*-LA compared to reactions catalyzed by $FeCl_3$, but THF yields were significantly decreased. We hypothesized that the lower THF yield was due to PEG-600, which is hygroscopic and able to coordinate to $FeCl_3$, thereby tempering its reactivity. To further increase the yield of both monomers during the reactive distillation reaction, the two catalysts were added sequentially to the reaction (Figure 5, columns 3-4). Extended reaction time (72 h) in the first step involving $ZnCl_2$/PEG-600 as the catalyst was required to achieve high *L*-LA recovery and high THF yield in the subsequent step (column 3). However, inverting the sequence of the two catalysts (i.e., $FeCl_3$ followed by $ZnCl_2$/PEG-600) was more effective, resulting in similar yields as observed when using $ZnCl_2$/PEG-600 first for both monomers but at significantly shorter reaction time (Figure 5, column 4). Finally, instead of carrying out the depolymerization in one pot, we isolated the polymer residue after $FeCl_3$ treatment, and then treated the resulting polymer with $ZnCl_2$/PEG-600 (Figure 5, column 5). Using this procedure, 78% of THF was isolated after $FeCl_3$ treatment; a more optimized distillation setup would likely yield near quantitative THF recovery. Moreover, ^{1}H NMR analysis of the polymer residue after the first step revealed pure PLLA without any evidence for poly(THF-*co*-CHO) or any detectable loss in tacticity from epimerization. Subsequent treatment of this polymer residue with $ZnCl_2$/PEG-600, resulted in 80% recovery of *L*-LA with similar optical purity as the *L*-LA used in the polymerization reaction.

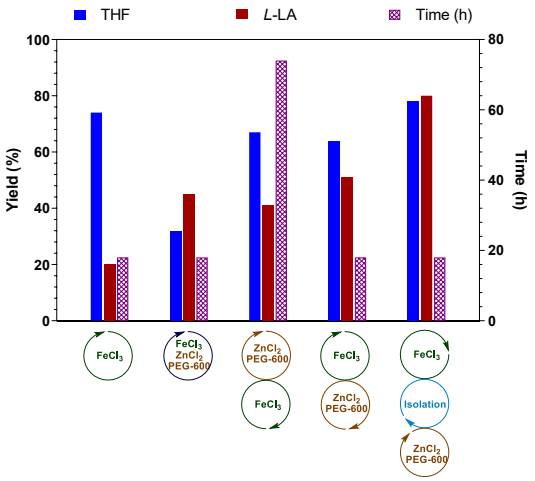

Figure 5. Depolymerization of triblock copolymer L-THF-L under different reactive distillation condition. Reaction time was controlled at 18 h (16 h for PLLA depolymerization and 2 h for polyTHF depolymerization) or 74 h (72 h for PLLA depolymerization and 2 h for polyTHF depolymerization).

Conclusion

In conclusion, a redox-switchable iron-based catalyst enabled the synthesis of A–B–A' and A–B–C triblock copolymers containing PLA end-blocks and poly(THF-*co*-CHO) mid-blocks. These unique polymers, derived entirely from commodity monomers, had modular compositions that could be altered by changing the ratio of monomers, the solvent used, and through sequential redox-reagent and monomer additions. The mechanical properties of the triblock copolymers demonstrated characteristics of TPEs with high flexibility observed in triblock copolymers that contained a high percentage of THF in the soft mid-block. Stereocomplexes obtained from blends of triblock copolymers containing PLLA and PDLA end-blocks further increased the T_m, flexibility, and toughness of the polymers. The triblock copolymers could be depolymerized under reactive distillation conditions with recovered yields of the constituent monomers exceeding 75% through sequential depolymerization with $FeCl_3$ followed by $ZnCl_2$/PEG-600 for the depolymerization of poly(THF) and PLA, respectively. These results demonstrate how redox-switchable polymerization reactions can be exploited to synthesize polymers that are difficult to access through other routes and illustrates how this polymerization method can be a valuable tool for chemically recyclable materials.

Acknowledgements

This research was financially supported by the NSF (CHE-1955926 and CHE-2003662). The data reported here was supported by the NIH-S10 (award 1S10OD026910-01A1) and the NSF-MRI (award CHE-2117246) Programs. The authors thank the Boston College Scientific Instrumentation & Machining Services for assistance with the work presented in this paper. Finally, the authors recognize the tragic death of Prof. Jeffrey A. Byers during the preparation of this manuscript. They acknowledge and miss his genuine collegiality, mentorship, and friendship.

Keywords: redox switchable catalysis • triblock copolymer • thermoplastic elastomer • chemical recycling

[1] A. J. Teator, D. N. Lastovickova, C. W. Bielawski, *Chem. Rev.* **2016**, *116*, 1969–1992.

[2] A. C. Deacy, G. L. Gregory, G. S. Sulley, T. T. D. Chen, C. K. Williams, *J. Am. Chem. Soc.* **2021**, *143*, 10021–10040.

[3] H. J. Yoon, J. Kuwabara, J.-H. Kim, C. A. Mirkin, *Science* **2010**, *330*, 66–69.

[4] C. K. A. Gregson, V. C. Gibson, N. J. Long, E. L. Marshall, P. J. Oxford, A. J. P. White, *J. Am. Chem. Soc.* **2006**, *128*, 7410–7411.

[5] E. M. Broderick, N. Guo, C. S. Vogel, C. Xu, J. Sutter, J. T. Miller, K. Meyer, P. Mehrkhodavandi, P. L. Diaconescu, *J. Am. Chem. Soc.* **2011**, *133*, 9278–9281.

[6] X. Wang, A. Thevenon, J. L. Brosmer, I. Yu, S. I. Khan, P. Mehrkhodavandi, P. L. Diaconescu, *J. Am. Chem. Soc.* **2014**, *136*, 11264–11267.

[7] M. Qi, H. Zhang, Q. Dong, J. Li, R. A. Musgrave, Y. Zhao, N. Dulock, D. Wang, J. A. Byers, *Chem. Sci.* **2021**, *12*, 9042–9052.

[8] M. Qi, Q. Dong, D. Wang, J. A. Byers, *J. Am. Chem. Soc.* **2018**, *140*, 5686–5690.

[9] A. B. Biernesser, K. R. Delle Chiaie, J. B. Curley, J. A. Byers, *Angew. Chem. Int. Ed.* **2016**, *55*, 5251–5254.

[10] Ashley B. Biernesser, B. Li, J. A. Byers, *J. Am. Chem. Soc.* **2013**, *135*, 16553–16560.

[11] A. Piermattei, S. Karthikeyan, R. P. Sijbesma, *Nat. Chem* **2009**, *1*, 133–137.

[12] P. Olsén, K. Odelius, H. Keul, A.-C. Albertsson, *Macromolecules* **2015**, *48*, 1703–1710.

[13] A. J. D. Magenau, N. C. Strandwitz, A. Gennaro, K. Matyjaszewski, *Science* **2011**, *332*, 81–84.

[14] B. M. Peterson, S. Lin, B. P. Fors, *J. Am. Chem. Soc.* **2018**, *140*, 2076–2079.

[15] J. Xu, K. Jung, A. Atme, S. Shanmugam, C. Boyer, *J. Am. Chem. Soc.* **2014**, *136*, 5508–5519.

[16] V. Kottisch, Q. Michaudel, B. P. Fors, *J. Am. Chem. Soc.* **2016**, *138*, 15535–15538.

[17] V. Kottisch, Q. Michaudel, B. P. Fors, *J. Am. Chem. Soc.* **2017**, *139*, 10665–10668.

[18] Q. Michaudel, T. Chauviré, V. Kottisch, M. J. Supej, K. J. Stawiasz, L. Shen, W. R. Zipfel, H. D. Abruña, J. H. Freed, B. P. Fors, *J. Am. Chem. Soc.* **2017**, *139*, 15530–15538.

[19] B. M. Neilson, C. W. Bielawski, *Chem. Commun.* **2013**, *49*, 5453.

[20] Z. C. Hern, S. M. Quan, R. Dai, A. Lai, Y. Wang, C. Liu, P. L. Diaconescu, *J. Am. Chem. Soc.* **2021**, *143*, 19802–19808.

[21] Y. Zhu, M. R. Radlauer, D. K. Schneiderman, M. S. P. Shaffer, M. A. Hillmyer, C. K. Williams, *Macromolecules* **2018**, *51*, 2466–2475.

[22] S. M. Quan, X. Wang, R. Zhang, P. L. Diaconescu, *Macromolecules* **2016**, *49*, 6768–6778.

[23] M. Abubekerov, J. Wei, K. R. Swartz, Z. Xie, Q. Pei, P. L. Diaconescu, *Chem. Sci.* **2018**, *9*, 2168–2178.

[24] J.-F. Lutz, M. Ouchi, D. R. Liu, M. Sawamoto, *Science* **2013**, *341*, 1238149.

[25] C. Romain, C. K. Williams, *Angew. Chem. Int. Ed.* **2014**, *53*, 1607–1610.

[26] Y. Zhu, C. Romain, C. K. Williams, *J. Am. Chem. Soc.* **2015**, *137*, 12179–12182.

[27] R. C. Jeske, A. M. DiCiccio, G. W. Coates, *J. Am. Chem. Soc.* **2007**, *129*, 11330–11331.

[28] K. Satoh, M. Matsuda, K. Nagai, M. Kamigaito, *J. Am. Chem. Soc.* **2010**, *132*, 10003–10005.

[29] J. Huang, S. R. Turner, *Polymer* **2017**, *116*, 572–586.

[30] E. Grune, T. Johann, M. Appold, C. Wahlen, J. Blankenburg, D. Leibig, A. H. E. Müller, M. Gallei, H. Frey, *Macromolecules* **2018**, *51*, 3527–3537.

[31] T. Soejima, K. Satoh, M. Kamigaito, *J. Am. Chem. Soc.* **2016**, *138*, 944–954.

[32] S. Pfeifer, J.-F. Lutz, *J. Am. Chem. Soc.* **2007**, *129*, 9542–9543.

[33] M. L. McGraw, R. W. Clarke, E. Y.-X. Chen, *J. Am. Chem. Soc.* **2020**, *142*, 5969–5973.

[34] S. Kernbichl, M. Reiter, J. Mock, B. Rieger, *Macromolecules* **2019**, *52*, 8476–8483.

[35] G. S. Sulley, G. L. Gregory, T. T. D. Chen, L. Peña Carrodeguas, G. Trott, A. Santmarti, K.-Y. Lee, N. J. Terrill, C. K. Williams, *J. Am. Chem. Soc.* **2020**, *142*, 4367–4378.

[36] T. T. D. Chen, L. P. Carrodeguas, G. S. Sulley, G. L. Gregory, C. K. Williams, *Angew. Chem. Int. Ed.* **2020**, *59*, 23450–23455.

[37] M. T. Martello, M. A. Hillmyer, *Macromolecules* **2011**, *44*, 8537–8545.

[38] M. A. Hillmyer, W. B. Tolman, *Acc. Chem. Res.* **2014**, *47*, 2390–2396.
[39] M. T. Martello, D. K. Schneiderman, M. A. Hillmyer, *ACS Sustainable Chem. Eng.* **2014**, *2*, 2519–2526.
[40] D. K. Schneiderman, E. M. Hill, M. T. Martello, M. A. Hillmyer, *Polym. Chem.* **2015**, *6*, 3641–3651.
[41] C. L. Wanamaker, L. E. O'Leary, N. A. Lynd, M. A. Hillmyer, W. B. Tolman, *Biomacromolecules* **2007**, *8*, 3634–3640.
[42] E.-M. Christ, J. Herzberger, M. Montigny, W. Tremel, H. Frey, *Macromolecules* **2016**, *49*, 3681–3695.
[43] W. Zhang, X. Fan, W. Tian, H. Chen, X. Zhu, H. Zhang, *RSC Adv.* **2015**, *5*, 66073–66081.
[44] A. Guo, W. Yang, F. Yang, R. Yu, Y. Wu, *Macromolecules* **2014**, *47*, 5450–5461.
[45] I. Asenjo-Sanz, A. Veloso, J. I. Miranda, A. Alegría, J. A. Pomposo, F. Barroso-Bujans, *Macromolecules* **2015**, *48*, 1664–1672.
[46] Y. Wang, E. J. Goethals, *Macromolecules* **2000**, *33*, 808–813.
[47] S. Yoshida, H. Suga, S. Seki, *Polym. J.* **1973**, *5*, 25–32.
[48] K. K. S. Hwang, G. Wu, S. B. Lin, S. L. Cooper, *J. Polym. Sci., Polym. Chem. Ed.* **1984**, *22*, 1677–1697.
[49] S. Enthaler, A. Trautner, *ChemSusChem* **2013**, *6*, 1334–1336.
[50] P. Majgaonkar, R. Hanich, F. Malz, R. Brüll, *Chem. Eng. J.* **2021**, *423*, 129952.
[51] D. Grewell, G. Srinivasan, E. Cochran, *J. Renew. Mater.* **2014**, *2*, 157–165.
[52] C. Alberti, S. Enthaler, *ChemistrySelect* **2020**, *5*, 14759–14763.
[53] M. N. Siddiqui, L. Kolokotsiou, E. Vouvoudi, H. H. Redhwi, A. A. Al-Arfaj, D. S. Achilias, *J. Polym. Environ.* **2020**, *28*, 1664–1672.
[54] L. A. Román-Ramírez, P. McKeown, C. Shah, J. Abraham, M. D. Jones, J. Wood, *Ind. Eng. Chem. Res.* **2020**, *59*, 11149–11156.
[55] E. Cheung, C. Alberti, S. Enthaler, *ChemistryOpen* **2020**, *9*, 1224–1228.
[56] M. Xiong, D. K. Schneiderman, F. S. Bates, M. A. Hillmyer, K. Zhang, *Proc. Natl. Acad. Sci. U. S. A.* **2014**, *111*, 8357–8362.
[57] C. Li, L. Wang, Q. Yan, F. Liu, Y. Shen, Z. Li, *Angew. Chem. Int. Ed.* **2022**, *61*, e202201407.
[58] D. K. Schneiderman, M. E. Vanderlaan, A. M. Mannion, T. R. Panthani, D. C. Batiste, J. Z. Wang, F. S. Bates, C. W. Macosko, M. A. Hillmyer, *ACS Macro Lett.* **2016**, *5*, 515–518.
[59] R. C. Burrows, B. F. Crowe, *J. Appl. Polym. Sci.* **1962**, *6*, 465–473.
[60] M. Inoue, A. Kanazawa, S. Aoshima, *Macromolecules* **2021**, *54*, 5124–5135.
[61] H. Tsuji, K. Osanai, Y. Arakawa, *Cryst. Growth Des.* **2018**, *18*, 6009–6019.
[62] E. M. Frick, M. A. Hillmyer, *Macromol. Rapid Commun.* **2000**, *21*, 1317–1322.
[63] M. Meier-Merziger, J. Imschweiler, F. Hartmann, B.-J. Niebuur, T. Kraus, M. Gallei, H. Frey, *Angew. Chem. Int. Ed.* **2023**, *62*, e202310519.
[64] C. Fang, X. Wang, X. Chen, Z. Wang, *Polym. Chem.* **2019**, *10*, 3610–3620.
[65] C. Zhou, Z. Wei, X. Lei, Y. Li, *RSC Adv.* **2016**, *6*, 63508–63514.
[66] S. Schüttner, C. Gardiner, F. S. Petrov, N. Fotaras, J. Preis, G. Floudas, H. Frey, *Macromolecules* **2023**, *56*, 8247–8259.
[67] Y. Li, C. Han, *Ind. Eng. Chem. Res.* **2012**, *51*, 15927–15935.
[68] M. Razavi, S.-Q. Wang, *Macromolecules* **2019**, *52,* 5429-5441.
[69] I. E. J. Kohn, *BIOMATERIALS* **1991**, *12*, 292–304.
[70] G. L. Gregory, G. S. Sulley, L. Peña Carrodeguas, T. T. D. Chen, A. Santmarti, N. J. Terrill, K.-Y. Lee, C. K. Williams, *Chem. Sci.* **2020**, *11*, 6567–6581.
[71] C. L. Wanamaker, M. J. Bluemle, L. M. Pitet, L. E. O'Leary, W. B. Tolman, M. A. Hillmyer, *BIOMACROMOLECULES* **2009**, *10*, 2904–2911.
[72] G. L. Gregory, G. S. Sulley, J. Kimpel, M. Łagodzińska, L. Häfele, L. P. Carrodeguas, C. K. Williams, *Angew. Chem. Int. Ed.* **2022**, *61*, e202210748.
[73] S. Nagarajan, K. Deepthi, E. B. Gowd, *Polymer* **2016**, *105*, 422–430.
[74] C. F. Gallin, W.-W. Lee, J. A. Byers, *Angew. Chem. Int. Ed.* **2023**, *62*, e202303762.

WILEY-VCH

Entry for the Table of Contents

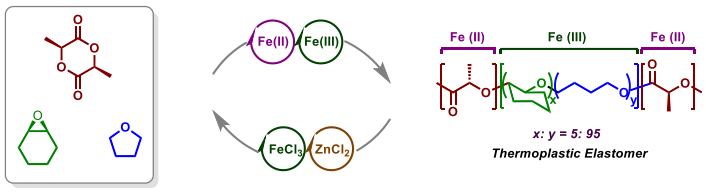

Triblock copolymers containing poly(*L*-lactic acid) hard blocks and poly(tetrahydrofuran-*co*-cyclohexene oxide) soft blocks were synthesized using redox-switchable catalysis. The polymers demonstrated improved flexibility and mechanical properties similar to thermoplastic elastomers and underwent depolymerization under reactive distillation using Lewis acid catalysts, showing the material can be chemically recycled for a circular plastics economy.

WILEY-VCH